Int. J. Heat Mass Transfer. Vol. 32, No. 3, pp. 585–593, 1989
Printed in Great Britain

0017–9310/89 $3.00 + 0.00

The effective thermal conductivity of high temperature particulate beds—I. Experimental determination

J. S. M. BOTTERILL, A. G. SALWAY† and Y. TEOMAN‡
Department of Chemical Engineering, University of Birmingham, P.O. Box 363, Birmingham B15 2TT, U.K.

(*Received* 12 *November* 1987 *and in final form* 16 *August* 1988)

Abstract—The experimental estimation of the effective thermal conductivities of packed beds of alumina of mean particle size 376 μm and sand of mean sizes 410 and 590 μm over the temperature range 400–950°C is described. The method used involves the measurement of the changing axial and radial temperature profiles through a cylindrical bed ~700 mm in diameter and high as it cooled. The effective bed thermal conductivity is estimated by fitting a suitable model to the profiles by regression analysis.

1. INTRODUCTION

THE EFFECTIVE thermal conductivity of particulate beds is of importance in many industrial operations including the design and operation of highly exothermic reactions in packed bed reactors, regenerative thermal operations and other high temperature heat storage systems. Although many models for the prediction of packed bed thermal conductivities have been proposed, they have not generally been tested over a wide range of temperatures. The first part of this paper describes experimental work which was undertaken to measure the effective thermal conductivity of packed beds of alumina and sand at temperatures up to 950°C. In the second part, the implications of the results are discussed in relation to some of the published models and their predictions. Fuller details are given elsewhere [1].

2. PRINCIPAL OF THE EXPERIMENT

Our original interest in the prediction of the effective thermal conductivity of packed beds arose from consideration of the use of particulate solids as a high temperature heat storage medium [2–5] for which their high heat capacity and low vapour pressure make them very attractive. Consequently, the method adopted for the measurement of effective thermal conductivity was also designed to test predictions for the behaviour of a particulate bed heat store. It involved the construction of a cylindrical storage unit containing a bed of approximately 700 mm diameter and height. The solids in this were first brought to a uniform high temperature by fluidizing them with an air–propane gas mixture burning within the bed. After attaining the required temperature, a carefully set up array of thermocouples mounted on a jig was located in the bed and the bed defluidized. As it cooled over a period of days, the changing axial and radial temperature profiles were logged. The effective bed thermal conductivity and, incidentally, the wall and surface heat fluxes were then estimated over the available range of temperatures by fitting a model to the changing temperature profiles using regression analysis.

3. THE EXPERIMENTAL SET-UP

An outline of the rig is shown in Fig. 1. The bed was contained within a cylindrical vessel of diameter 690 mm, depth 900 mm and with a wall thickness of 6.3 mm fabricated from 37/18 nickel–chrome steel to withstand the burning air–gas mixture. The distributor plate was made of porous ceramic tile and this and the plenum chamber beneath were divided into three segmental compartments in order to minimize the volume of premixed gases in case of a flashback. The gas mixers were designed to provide a maximum of 2.2 kg h^{-1} of propane in the gas stream against a back pressure of up to 136 kN m^{-2} with a supply line pressure of 205 kN m^{-2}. There was an air cooling ring around the perimeter of the distributor to reduce thermal stresses there.

A number of chromel–alumel thermocouples were inserted through the vessel wall and six 6 mm diameter thermocouples were also positioned to touch the distributor plate in order to be able to monitor the temperature distribution around the containing surface (particularly during the heating up phase of the experiment). The outer surface of the stainless steel vessel was lagged with two layers of 25.4 mm thick Triton fibre blanket (thermal conductivity, 0.12 W

† Now at Department of Trade and Industry, Warren Spring Laboratory, Stevenage, Herts, U.K.
‡ Now at Türkiye şişe ve Cam Fabrikalari A.Ş., Istanbul, Turkey.

NOMENCLATURE

C specific heat of the solids [J kg^{-1} K^{-1}]
h overall wall heat transfer coefficient [W m^{-2} K^{-1}]
I number of temperatures measured
J number of parameters
k_e effective thermal conductivity of the bed [W m^{-1} K^{-1}]
q heat flux through bed top surface [W m^{-2}]
r radial coordinate [m]
R bed radius [m]
t time [s]
t_f duration of one-dimensional cooling [s]
T temperature [K]
T_1 initial axial temperature profile [K]
T_2 initial radial temperature profile [K]
T_e surroundings temperature [K]
$\mathbf{X}$ sensitivity matrix
z axial coordinate [m]
Z bed half length [m].

Greek symbols
β_j parameters in polynomials representing the effective thermal conductivity and boundary heat fluxes
ε bed voidage
η_i temperatures predicted by the model corresponding to those measured [K]
ρ bulk density of the bed [kg m^{-3}]
ϕ particle shape factor.

m^{-1} K^{-1}) and a further layer of Rockwool lagging 50 mm thick.

The freeboard of the bed was enclosed and the exhaust gases were extracted through a cowling over the top. Access was available through the enclosure for the insertion of the array of thermocouples which were to be used to measure the changing thermal profiles through the bed. A pilot torch was mounted on the rim of the vessel to ignite the air–gas mixture at start-up and to maintain a source of ignition should there be a loss of flame while the bed was being supplied with the air–gas mixture.

Combustion air was supplied by a Rootes blower powered by a 7.5 kW electric motor. The blower could deliver up to 0.138 m^3 s^{-1} at 0°C and 101.3 kN m^{-2}. When the bed was operating at 900°C, the flow rate required was of the order of 0.01 m^3 s^{-1} (0°C, 101.3 kN m^{-2}). The air flow rate to the bed was controlled by a by-pass valve and measured using orifice plates designed according to the British Standard. The propane gas was obtained from three 47.6 kg cylinders housed in a compound outside the laboratory (three were necessary as there was a danger of the liquified gas freezing if the abstraction rate from an individual bottle was too high). Safety devices operated a solenoid valve in the gas supply line should the temperature in the plenum chamber rise too high, or there be a failure of the air supply or should the pilot torch go out. A gas detector was also included in the system to shut off the gas supply should there be any build up of propane at floor level from leakage. The whole could be shut down by emergency buttons close to the exits from the laboratory.

To measure the developing temperature profiles during the course of cooling, a carefully positioned array of thermocouples mounted on an 18/8 stainless steel frame (Fig. 2) was used. The chromel–alumel thermocouples were 700 mm long and 3 mm in diam-

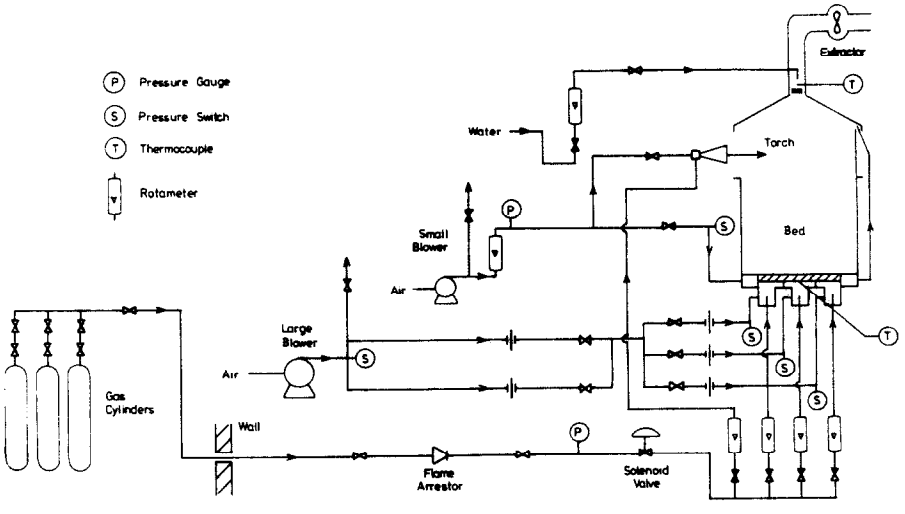

FIG. 1. Schematic diagram of rig.

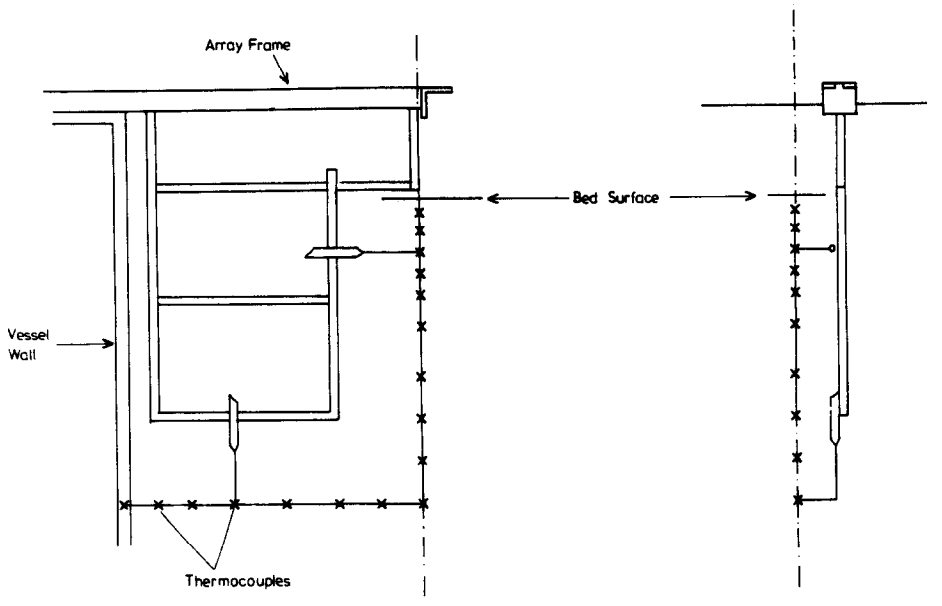

FIG. 2. Array in position.

eter except that the final 100 mm of each was swaged down to a diameter of 1.0 mm. The object of this was to produce a relatively robust thermocouple which did not create undue thermal disturbance at the temperature measuring point. The array thermocouples projected from the frame and were positioned so that when the array was located in the bed, the junctions lay in two lines, one along the vertical bed axis to a depth of 350 mm below the bed surface and the other radially at that depth beneath the surface. The thermocouples were bent at right angles from the frame at about 50 mm from the junction so that they were perpendicular to the direction of heat flow and lying along approximately isothermal planes to minimize conduction along their sheaths. The jig carrying the array was counterbalanced by a weight and arranged to slide along a rail above the bed. It entered through a slot in the cowling and freeboard enclosure to locate against a vertical rod. When in position over the bed it could be freed from the rail and lowered and positioned accurately at the required location within the bed. The counterbalance was then disconnected.

Connections from the thermocouples were carried back using further chromel–alumel wires to a Datron logging system controlled by a 2001-32N Commodore Pet computer. This employed a Datron Autocal 1061 digital voltmeter and a Datron 1220 scanner. It had a capacity of 60 channels. A program was written to operate the logger which allowed for the periodic sampling of all the thermocouples and for the measured temperatures to be displayed on the Pet screen, printed out and recorded on tape.

4. EXPERIMENTAL PROCEDURE

Closely sized samples of sand (mean diameter 410 and 590 μm) and alumina (376 μm) were used in the experimental tests. The sieve analyses and physical properties of the samples are given in Tables 1 and 2, respectively. The mean particle sizes quoted were calculated according to equation (14) in Part II. Before beginning the experiment, the array of thermocouples had to be set accurately at the desired spacings so that the junctions would lie along the bed axis and the radius passing through a wall mounted

Table 1. Sieve analyses of the alumina and silica sand samples

Sieve size (μm)	Cumulative weight %		
	376 μm alumina	410 μm silica	590 μm silica
125	—	—	—
150	0.10	0.1	—
178	0.16	0.16	—
211	0.26	0.30	—
353	25.92	17.02	0.47
500	99.21	78.56	14.1
600	99.93	99.57	32.0
699	99.97	99.98	92.9
743	100.00	—	98.83
853	—	100.0	99.80
955	—	—	99.96
1040	—	—	100.00

Table 2. Properties of the bed materials

	Mean particle size (μm)	Voidage, ε	Apparent bulk density (kg m^{-3})	Shape factor,† ϕ
Sand	410	0.428	1512	0.9
Sand	590	0.431	1504	0.88
Alumina	376	0.54	1848	0.88

† The shape factors were estimated by measuring the minimum fluidizing velocities of the materials and using the Ergun equation [12].

thermocouple when finally located within the bed (Fig. 2). The bed of particles was prepared by fluidizing it. Propane was mixed with the fluidizing air and the mixture ignited above the bed. Initially the bed heated up by back radiation and the flame front then travelled down into the bed which, during the early stages, was only intermittently fluidized. The thermocouples mounted in the vessel wall were particularly useful in gauging the progress of this. (If fluidization was maintained continuously through the initial heating period, the bulk bed temperature fell below that at which combustion could be sustained within any zone of the bed.) Once above 700°C combustion could be maintained within the bed and the bed was then vigorously fluidized in order to bring it as close to an isothermal condition as possible. Even so there remained minor temperature differences throughout the bulk of the bed (largely because of the disturbance to fluidization caused by the cooling ring provided to reduce stresses at the perimeter of the distributor). These were significant in their effect on the method of analysis of the data as mentioned below.

Once the bed was as nearly isothermal as could be achieved at the desired temperature, the gas flow rate was reduced to bring the bed back just to the point of fluidization to reduce possible disturbance to the spacing of the array of thermocouples as they were inserted precisely within the bed. The bed was then quickly defluidized and the cooling experiment begun.

5. ANALYSIS OF DATA

The method of non-linear parameter estimation was used to estimate the effective thermal conductivity of the bed from the changing temperature profiles as the bed cooled. It was necessary to construct a mathematical model of the cooling process. This involved the solution of the non-linear transient heat conduction equation taking into account the strong temperature dependence of the bed's effective thermal conductivity, specific heat capacity and of the wall and top surface heat fluxes. The problem was simplified assuming cylindrical symmetry and by using two one-dimensional models to calculate the radial and axial profiles rather than a single two-dimensional model. Since the initial temperature of the core of the bed is approximately uniform, the development of the radial temperature profile may be considered to be one-dimensional until the temperature penetration depth is of the order of the radius; the core temperature should remain virtually constant for the first 5–6 h of cooling. Similarly, the profile along the axis would also be closely one-dimensional.

The radial profile was calculated from the following model:

$$\rho C\frac{\partial T}{\partial t}=\frac{k_e}{r}\frac{\partial T}{\partial r}+\frac{\partial}{\partial r}\left(k_e\frac{\partial T}{\partial r}\right),\quad 0<t\leqslant t_f,\quad 0\leqslant r\leqslant R \tag{1}$$

$$-k_e\frac{\partial T}{\partial r}=h(T-T_c),\quad r=R,\quad t>0 \tag{2}$$

$$T(r,0)=T_2(r) \tag{3}$$

where $T(r,t)$, $k_e(T)$, $C(T)$, $h(T)$.

Equations (1)–(3) were solved by a Crank–Nicholson finite difference method using the approximations for non-linear parabolic equations of Mitchell and Griffiths [6]. The resulting sets of simultaneous equations were solved by Liebmann's successive over relaxation method, the temperatures at the grid points being iterated until convergence was obtained. At each iteration the thermal properties at the grid points were re-evaluated for the latest temperature profile. The specific heat capacities of the alumina and silica were calculated by interpolation from experimental data taken from the literature. The data of Shomate and Naylor [7] was used for alumina whilst data was taken from three sources for the silica. Up to 500°C values were taken from Moser [8] and Sinel'nikov [9]; from 525 to 600°C that of Sinel'nikov was used and above 620°C the data of Leonidov *et al.* [10] was used. The specific heat capacity of silica exhibits a discontinuity at the transition between α quartz and β quartz which takes place at 573°C. Since the programme used numerical interpolation to estimate the specific heats at the required temperatures, there was no difficulty in dealing with this discontinuity. A 21 point grid with a time step of 112.5 s was used. The effective thermal conductivity, surface and wall heat transfer coefficients were expressed as polynomials, the coefficients of which were the parameters to be estimated. A simple least squares function, calculated from the measured temperature profiles and the predicted profiles from the solution of the model, was minimized. Gauss' method of search was used together with the modified Box–Kanemasu interpolation method to prevent overshooting the minimum. The derivatives required were evaluated numerically. The lengthy calculations were carried out on a CDC 7600 computer.

The axial profile was analysed by the same method except that the model equations were

$$\rho C\frac{\partial T}{\partial t}=\frac{\partial}{\partial z}\left(k_e\frac{\partial T}{\partial z}\right),\quad 0<t\leqslant t_f,\quad 0\leqslant z\leqslant Z \tag{4}$$

$$-k_e\frac{\partial T}{\partial z}=q(T),\quad z=Z,\quad t>0 \tag{5}$$

$$\frac{\partial T}{\partial z}=0,\quad z=0,\quad t>0 \tag{6}$$

$$T(Z,0)=T_1(z) \tag{7}$$

where $T(z,t)$, $k_e(T)$, $C(T)$, $q(T)$.

6. EXPERIMENTAL RESULTS AND THEIR EVALUATION

The data used in the calculations were determined from the measurements logged by the data logger and

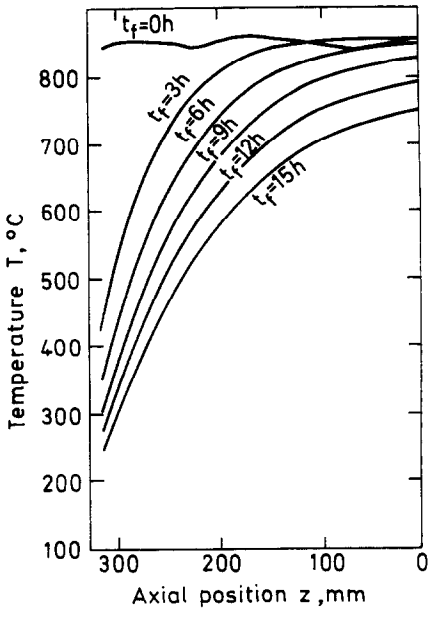

FIG. 3. Axial temperature profiles, 410 μm diameter sand bed.

the measured thermocouple spacing in the arrays. A typical series of axial temperature profiles drawn from the data for an experiment with 410 μm mean diameter sand is shown in Fig. 3. The profiles shown for times greater than about 6 h are increasingly two-dimensional and were not used in the analysis. The finite difference models used in the evaluation of the effective thermal conductivity, surface and wall heat flux polynomials require an initial temperature distribution as the starting point. This was found by plotting the initial profiles and drawing smooth curves through the data for the axial and radial profiles. The temperature at each of the 21 grid points for each profile was then read from the graph.

As noted above, the bed was vigorously fluidized to bring it as close as practicable to an isothermal condition after it has been heated up to the desired temperature before the array was inserted. Nevertheless, after insertion of the measuring array, slumping the bed and beginning to log the progress of cooling, some of the thermocouples, and particularly near the core region, registered small temperature rises (<5 K) showing that the bed was not initially perfectly isothermal (Fig. 3). The one-dimensional analysis could not cope with these local two-dimensional effects so it was necessary to choose the initial conditions at a later time when all the thermocouples were recording falling temperatures and the initial hot spots had evened out. That such small temperature changes detected by the thermocouples near the centre of the bed should be so important is probably due to the shape of the analysed profiles. From the nature of the cooling process, most of the measurements lie in the centre of the temperature range. A smaller number of measurements towards the surface of the bed influence the lower temperature estimates of the effective thermal conductivity but these exhibit the greatest temperature range. It is data from the thermocouples near the core which particularly influences the high temperature range prediction. In this region, because of the initial hot spots, the estimated effective thermal conductivity exhibited a maximum, increasing and then falling as the temperature increased. However, by choosing a later initial condition for which all the recorded temperature changes were falling, this anomalous behaviour of the estimates disappeared.

The magnitude of the errors incurred by the assumption of a one-dimensional cooling model was examined by progressively extending the time over which the data was analysed. This is illustrated in Fig. 4 where data collected over 4, 5 and 6 h from an experiment with a bed of 376 μm alumina was analysed. As would be expected, there is a slight rise in the estimated conductivity as the analysis period increases but the error is not large compared with the value of the thermal conductivity. It is greater at the ends of the temperature range than in the middle. If the period is extended beyond 7 h there are convergence problems because of the increasing difficulty in trying to fit the two-dimensional character of the resulting profiles to a one-dimensional model.

Because of the ejection of material from the bed when it was being fluidized vigorously to produce as nearly isothermal conditions as possible during the final stage of preparation, it could happen that the top thermocouple was just proud of the bed surface when the bed was slumped. In such cases, the measurements from the thermocouple were excluded from the analysis. The temperature profile near the surface was always steep which made it impossible to deduce the initial condition all the way up to the bed surface. This difficulty was overcome by prescribing the boundary conditions on an imaginary plane passing through the topmost thermocouple in the bed. In this way, the initial condition was known up to the boundary. The thermal conductivity variation and the heat flux through the imaginary plane were then estimated.

An additional effect was that of the differential expansion between the bed container carrying the array of thermocouples, the frame to which the array was finally secured and the bed. Thus, as the bed cools, the vessel, the bed and the array contract at different rates. In particular, the bed surface descended relative to the array during the course of cooling. To check on this, an indicator was fastened to the array from which the bed surface could more readily be gauged. Over the period for which data was collected for the analysis reported in this paper, however, no detectable movement was observed. Over the whole cooling period the apparent shrinkage appeared to be nonuniform and was probably due to intermittent settling after periods of differential movement between the bed and container.

The position of the thermocouples could only be measured when the bed was cold. Besides the measurements entailed in setting up the array at the beginning

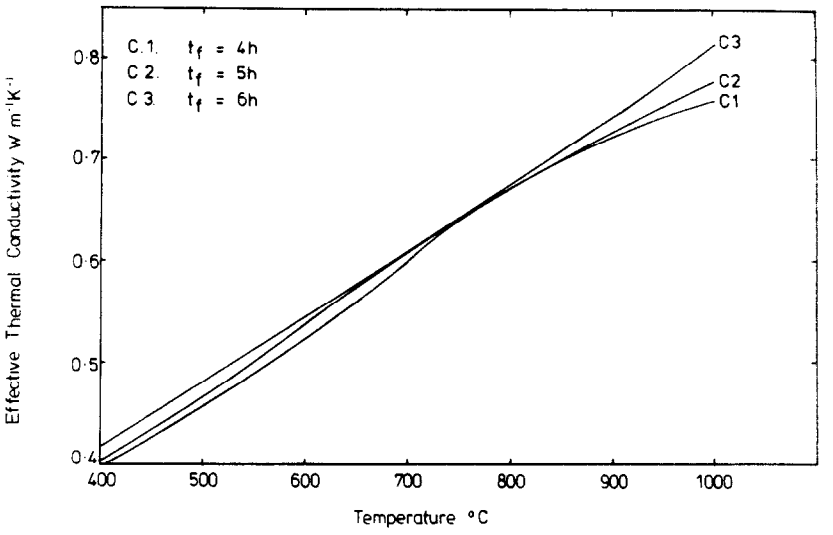

FIG. 4. Effect of analysis time on the effective thermal conductivity estimates; based on axial profiles for 376 μm alumina.

of the experiment, the sand was also carefully removed using a vacuum cleaner after an experiment so that the array could be removed without further disturbance of its configuration and the position of the thermocouples re-checked. In certain instances there was evidence of serious displacement and the data collected was discarded. Where slight movement had occurred, the measurements taken after the experiment were used on the assumption that the movement had been caused when the array was inserted and the bed slumped. Movement of couples in the direction of heat flow presented no problem but movements perpendicular to the heat flow, if large, could not be dealt with because the analysis required that all the thermocouples should be in a straight line. As a check on the possible error incurred through differential movement, the hot position of the thermocouples were calculated from the cold measurements of thermocouple spacing and expansion data for the 18/8 stainless steel of the array support. The estimated change in overall length of the array was about 1.8%. Analysis of alumina data for the two sets of spacings (Fig. 5) showed that thermal conductivity estimates from the hot positions were slightly higher but not markedly so. In both instances the fit obtained was good, the variance being 0.86 K^2 for the measured cold positions and 0.84 K^2 for the estimated hot positions.

Because the side of the containing cylinder was lagged whereas the top surface of the bed was free, the temperature change over the analysis period was considerably less with the radial data. Consequently the temperature changes on which the radial estimates are based are less and their overall accuracy is less than with the axial profiles. The range of temperature

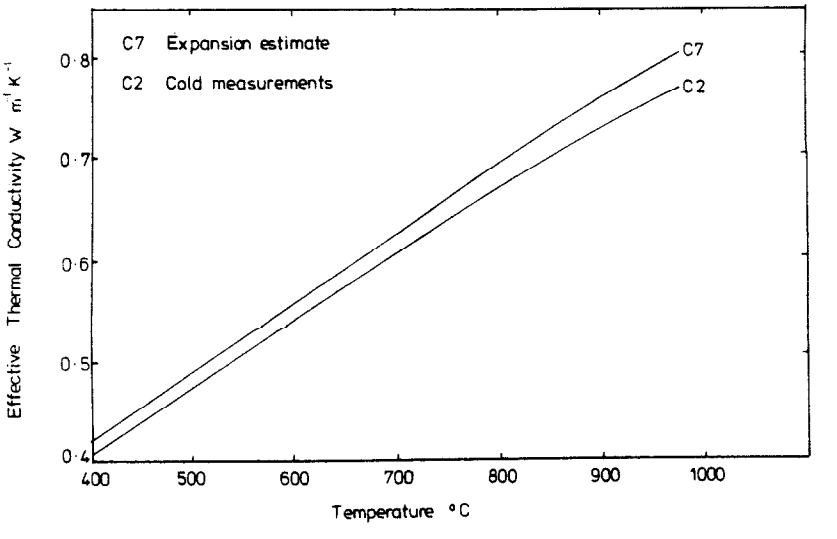

FIG. 5. Possible effect of expansion on the thermal conductivity estimates; based on axial profiles for 376 μm alumina and t_f = 5 h.

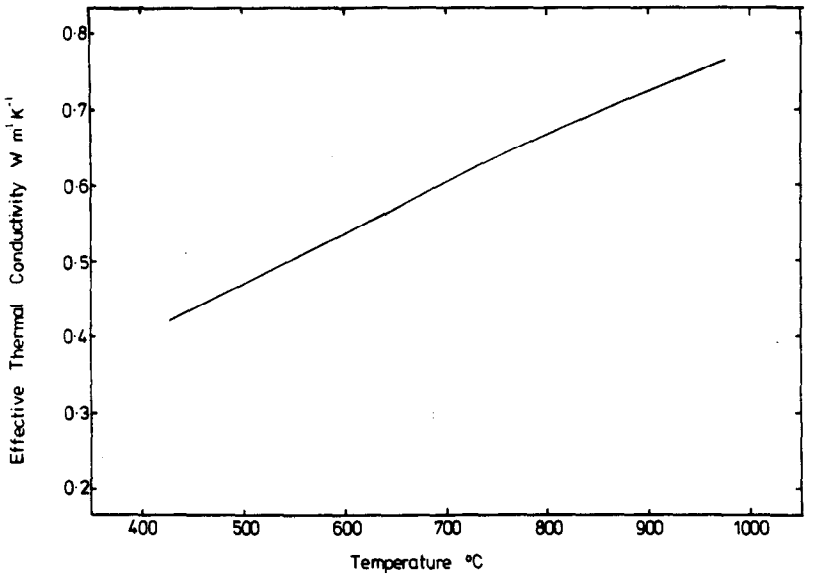

FIG. 6. Estimated effective thermal conductivity for bed of 376 μm alumina.

over which effective thermal conductivities could be estimated was also narrower for the radial data.

The Gauss search method used to minimize the least squares function is an iterative procedure. At each iteration it is necessary to calculate a Jacobian matrix defined as

$$X_{ij} = \frac{\partial \eta_i}{\partial \beta_j}, \quad i = 1, \ldots, I, \quad j = 1, \ldots, J \qquad (8)$$

in order to calculate an improved estimate of the parameters β_j. Here, the η_i are the temperatures predicted by the model for the estimated parameter values and the X_{ij} are known as sensitivity coefficients. If **X** has approximately linearly dependent columns the minimization problem will be ill conditioned; the minimum will be hard to locate and the uncertainty in the final estimate will be increased [11].

Inspection of the sensitivity coefficient showed that the minimization was poorly conditioned and that the ill conditioning was worse in the radial analysis than the axial. It was found necessary to use an interpolation procedure to improve convergence. Also the magnitude of the axial sensitivity coefficients was greater than with the radial ones, suggesting that for the axial case, the predicted temperatures were more sensitive to variation in the model parameters than for the radial case.

From the arguments outlined above, it is to be

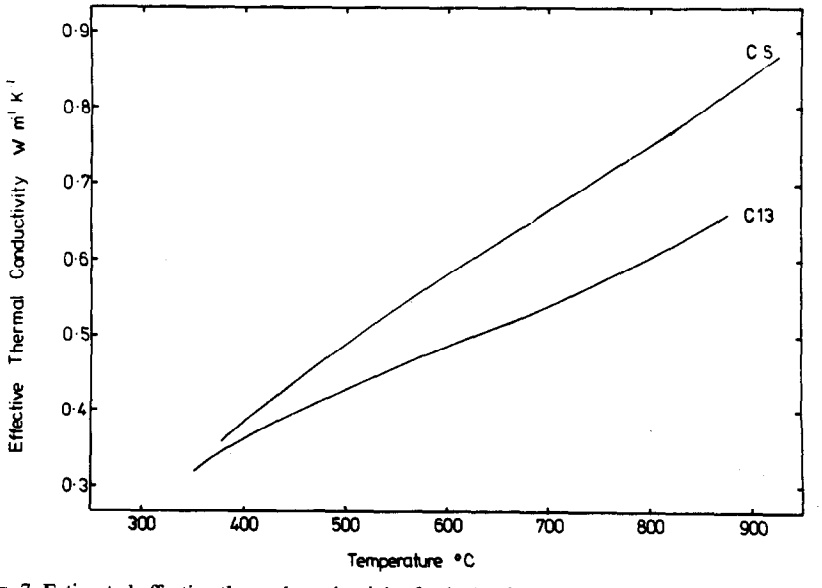

FIG. 7. Estimated effective thermal conductivity for beds of silica sand: (i) 410 μm; (ii) 590 μm.

expected, therefore, that the estimates taken from analyses of the axial profiles will be more accurate than those from the radial profiles and it is estimates based on the axial profile data which are presented in Figs. 6 and 7. Error due to two-dimensional heat flow is decreased as the analysis time span is reduced but the number of measurements analysed is also reduced with a consequent reduction both in the temperature range covered and the accuracy of the estimates. Accordingly, data sampled between 1 and 5 h after the commencement of cooling were chosen to represent the changing effective thermal conductivities for the 376 μm alumina (Fig. 6) and 590 μm silica sand (Fig. 7). The curve calculated for the 410 μm sand (Fig. 7) used data sampled between 3 and 6 h after the bed began to cool. The approximate method for the estimation of errors given by Beck and Arnold [11] gave extremely narrow confidence regions. However, this did not take into account errors inherent in the experimental procedures and the one-dimensional analysis of the data resulting from:

(a) the onset of two-dimensional heat flow as the experiment progresses;

(b) the difficulty involved in estimating the precise thermocouple locations (in particular, the analysis assumed that the thermocouples lay in a straight line but this was definitely not so for some runs as noted above and the data from these had to be discounted, otherwise the deviation was small);

(c) the movement of thermocouples because of relative expansion and contraction of the vessel and bed.

These are likely to be the major source of error and have been shown above to be significant but not too large. The effect of neglecting (a) above will be to overestimate the thermal conductivity and that of (c) to underestimate it. These calculations suggest that the best set of data was for the alumina experiment (Fig. 6). Over the whole range, the error is gauged to be less than ± 0.03 W m^{-1} K^{-1}. The 590 μm sand estimates (Fig. 7) are not so good. The estimated variances are higher and the spread of the calculated curves is greater. In the regions 350–550°C and 850–930°C the error is probably ± 0.05 W m^{-1} K^{-1}. In the central region it will be less than this.

7. CONCLUSIONS

The experimentally estimated values for the effective thermal conductivity of a packed bed of 376 μm mean particle diameter alumina are given in Fig. 6. The error in this is gauged to be less than 0.03 W m^{-1} K^{-1} over the whole range. For the sand experiments (Fig. 7) the errors are higher probably being up to 0.05 W m^{-1} K^{-1} for the 590 μm sand.

Acknowledgements—The support of SERC for this work is gratefully acknowledged together with that of computing facilities at Birmingham University and the University of Manchester Regional Computing Centre.

REFERENCES

1. A. G. Salway, The effective thermal conductivity of high temperature particulate beds, Ph.D. thesis, Birmingham University (1983).
2. J. S. M. Botterill and D. E. Elliott, Fluidized beds: answer to peak power, *Engineering* **198**, 146–147 (31 July 1964).
3. M. A. Bergougnou, J. S. M. Botterill, J. R. Howard, D. C. Newey, A. G. Salway and Y. Teoman, High temperature heat storage, Third International Conference on "Future Energy Concepts", London, 27–30 January 1981, I.E.E. Conference Publication, No. 192, pp. 61–64 (1981).
4. J. S. M. Botterill, A. G. Salway and Y. Teoman, Heat losses from a high temperature particulate bed store, International Conference on Energy Storage, Brighton, 29 April–1 May, pp. 101–112. BHRA (1981).
5. J. S. M. Botterill, A. G. Salway and Y. Teoman, High temperature heat storage, I.Chem.E. Symp. Series No. 78, "Energy, Money, Material Engineering", pp. A1–A7 (1982).
6. A. R. Mitchell and D. F. Griffiths, *The Finite Difference Method in Partial Differential Equations*. Wiley, Chichester (1978).
7. C. H. Shomate and B. F. Naylor, High temperature heat contents of aluminium oxide, aluminium sulfate, potassium sulfate, ammonium sulfate and ammonium bisulfate, *J. Am. Chem. Soc.* **67**(1), 72–75 (1945).
8. H. von Moser, Messung der wahren spezifischen Wärme von Silber, Nickel, β-Messing, Quarzkristall und Quarzglas zwischen 50 und 700°C nach einer verfeinten Methode, *Phys. Z.* **37**(21), 737–753 (1963).
9. N. N. Sinel'nikov, *Dokl. Akad. Nauk. S.S.R.* **92**, 369–372 (1953).
10. V. Y. Leonidov, Y. P. Barsku and N. Z. Khitarov, Determination of the heat capacity of kyanite and quartz at high temperatures by the method of thermal analysis, *Geokhimya* **5**, 414–419 (1964).
11. J. V. Beck and K. J. Arnold, *Parameter Estimation in Engineering and Science*. Wiley, New York (1977).
12. S. Ergun, Fluid flow through packed columns, *Chem. Engng Prog.* **48**, 89–94 (February 1952).

CONDUCTIVITE THERMIQUE EFFECTIVE DES LITS PARTICULAIRES A HAUTE TEMPERATURE—I. DETERMINATION EXPERIMENTALE

Résumé—On décrit la détermination expérimentale de la conductivitié thermique effective de lits fixes de paticules d'aluminium dont la taille moyenne est de 376 μm et de sable dont la grosseur moyenne est 410 et 590 μm, pour un domaine de température de 400 à 950°C. La méthode utilisée est basée sur la mesure du changement des profils de température axiaux et radiaux à travers un lit cylindrique de 700 mm de diamètre et de hauteur, pendant le refroidissement. La conductivité thermique effective du lit est estimée par calage sur une modélisation des profils par l'analyse de régression.

DIE EFFEKTIVE WÄRMELEITFÄHIGKEIT VON SCHÜTTUNGEN BEI HOHEN TEMPERATUREN—I. EXPERIMENTELLE BESTIMMUNG

Zusammenfassung—Beschrieben wird die Messung der effektiven Wärmeleitfähigkeit von Schüttungen aus Aluminium mit einer durchschnittlichen Partikelgröße von 376 μm und Sand mit 410 und 590 μm im Temperaturbereich 400–950°C. Gemessen wird die Änderung des radialen und axialen Temperaturprofils bei Kühlung einer zylindrischen Schüttung, deren Durchmesser bzw. Höhe ungefähr 700 mm mißt. Die effektive Wärmeleifähigkeit der Schüttung wird durch Anpassung eines geeigneten Modells an die Profile durch Regressionsanalyse berechnet.